Submitted to *Geophys. Res. Lett.*, January 2005

Polar processing and development of the 2004 Antarctic ozone hole: First results from Aura MLS

M. L. Santee,[1] G. L. Manney,[1,2] N. J. Livesey,[1] L. Froidevaux,[1] H. C. Pumphrey,[3] W. G. Read[1], M. J. Schwartz,[1] and J. W. Waters[1]

Abstract. The Microwave Limb Sounder (MLS) on Aura is providing an extensive dataset on stratospheric winter polar processing, including the first daily global observations of HCl, together with simultaneous measurements of ClO, HNO_3, H_2O, O_3, N_2O, and temperature (among others). We present first results charting the evolution of these quantities during the 2004 Antarctic late winter. Their behavior appears to be consistent with current understanding of the dominant processes affecting stratospheric O_3 in the Antarctic late winter.

1. Introduction

Aura, NASA's latest Earth Observing System (EOS) satellite, was launched 15 July 2004 into a 705-km, sun-synchronous, near-polar orbit [*Schoeberl et al.*, 2004]. One of its four instruments is the Microwave Limb Sounder (MLS), a greatly enhanced follow-on to the MLS instrument onboard the Upper Atmosphere Research Satellite (UARS) [e.g., *Waters et al.*, 1999]. EOS MLS improvements include better horizontal resolution and better precision and/or vertical resolution. In addition, unlike its predecessor, EOS MLS measures from 82°N to 82°S on every orbit, affording continuous monitoring of both polar regions. Perhaps most importantly, EOS MLS makes several measurements not available from UARS MLS, including the first daily global HCl profiles. Other EOS MLS observations relevant to polar process studies include ClO, HNO_3, H_2O, O_3, N_2O (also a new measurement for MLS) and temperature (T). Aura launched in time for MLS to observe the 2004 Antarctic late winter. Here we present first results from this period, with a focus on chlorine deactivation and ozone loss. Because of yaw maneuvers and other data gaps, UARS MLS never captured the complete chlorine deactivation period in the Antarctic. Studies of chlorine deactivation based on UARS data were also hampered by the lack of colocated ClO and HCl data, since MLS and the Halogen Occultation Experiment did not sample inside the Antarctic winter polar vortex simultaneously [*Douglass et al.*, 1995; *Santee et al.*, 1996].

Results shown here are from preliminary data processing algorithms. Instrument noise (precision) is not a significant contributor to the uncertainty in the averages used in these analyses. Over the latitude and altitude range of interest, the preliminary retrievals have a vertical resolution of 3–5 km and provisional estimated accuracies of about 2 K, 30 ppbv, 2 ppbv, 1 ppmv, 0.2 ppbv, 0.2 ppbv and 0.5 ppmv for T, N_2O, HNO_3, H_2O, HCl, ClO, and O_3, respectively. Refinements to the algorithms and extensive validation efforts are underway.

[1]Jet Propulsion Laboratory, California Institute of Technology, Pasadena.
[2]Department of Natural Sciences, New Mexico Highlands University.
[3]School of GeoSciences, The University of Edinburgh, UK.

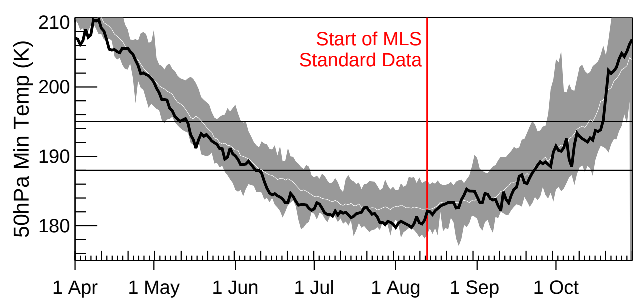

Figure 1. 50 hPa minimum temperatures poleward of 40°S from the National Centers for Environmental Prediction/Climate Prediction Center analyses during the 2004 Antarctic winter (black line). Grey shading shows the range over the 1979 to 2003 Antarctic winters, with the white line the average. Horizontal lines denote approximate existence thresholds for polar stratospheric clouds (PSCs) at 50 hPa.

2. The 2004 Antarctic Late Winter

Although lower stratospheric minimum temperatures were below average over most of the 2004 Antarctic winter, they rose and remained near average values after MLS began science operations in mid-August (Figure 1). The lower stratosphere warmed rapidly in September, halting further hetero-

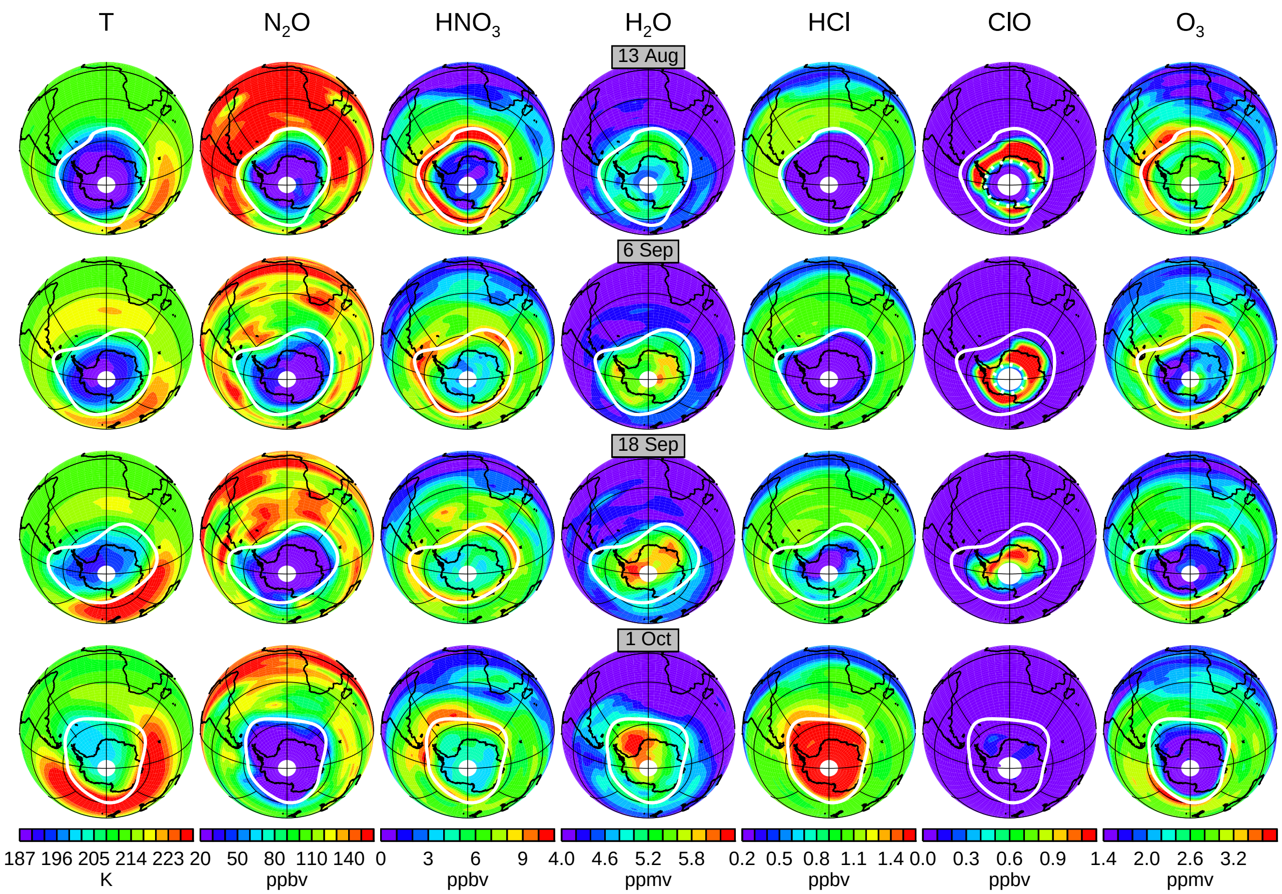

Figure 2. MLS T, N_2O, HNO_3, H_2O, HCl, ClO, and O_3 maps for selected days during the 2004 Antarctic late winter. MLS data were interpolated to 520 K ($\sim$20–22 km, 46 hPa) using Global Modeling and Assimilation Office Goddard Earth Observing System (GEOS-4) temperatures. Solid white lines show the 0.5×10^{-4} K m^2 kg^{-1} s^{-1} GEOS-4 potential vorticity (PV) contour, approximating the polar vortex boundary. Only data from the "day" (ascending) side of the orbit are shown for ClO; the dashed white circle on ClO maps demarks the edge of daylight.

geneous processing of vortex air by the end of the month.

An overview of the changes over the 2004 Antarctic late winter in key polar processing parameters measured by MLS at 520 K potential temperature is shown in Figure 2. The late-winter evolution of T, HNO_3, HCl, ClO, and O_3 at a slightly higher altitude (550 K) is presented in an animation provided as supplementary material. We start with 13 August, the first full day that MLS was operated in science mode. The long-lived tracer N_2O exhibits very low mixing ratios inside the polar vortex. Confined diabatic descent leads to low values of N_2O in the lower stratospheric vortex, but high values of species such as HNO_3 and H_2O whose concentrations increase with altitude in the lower stratosphere. In the coldest part of the vortex, however, gas-phase HNO_3 and H_2O have been substantially depleted as polar stratospheric clouds (PSCs) have formed. Heterogeneous chemical reactions on the surfaces of PSC particles convert chlorine from reservoir species, such as HCl, into active forms, primarily ClO. By mid-August, virtually all vortex HCl has been depleted, leading to significantly enhanced ClO. However, because measurements on the "day" (ascending) side of the orbit are made in late afternoon ($\sim$15:00–18:00 local solar time) at high southern latitudes, MLS is not capturing maximum ClO abundances, which occur around midday. ClO is not enhanced in the vortex core, which is still in polar night at this time. ClO is also not enhanced along the vortex edge, which is a characteristic pattern at 520 K seen in all southern hemisphere winters observed by UARS MLS [*Santee et al.*, 2003]. Finally, O_3 is significantly depleted in a ring roughly coinciding with the sunlit area of high ClO; this is consistent with studies showing that O_3 loss propagates poleward with the terminator, with little mixing between the vortex edge and core at this time [e.g., *Lee et al.*, 2000].

The region with temperatures low enough for PSCs has shrunk substantially by 6 September, and HNO_3 and H_2O have partially recovered. Some PSCs may have evaporated and released HNO_3 and H_2O back to the gas phase; continuing descent also contributes to the observed increases. HCl remains very low throughout the vortex, and ClO has increased in the vortex core with exposure to daylight. Ozone depletion has progressed throughout most of the vortex, since mixing ratios have decreased despite replenishment by downward transport. By just 12 days later, on 18 September, chlorine partitioning has changed considerably: HCl has started to recover over most of the vortex, and ClO is much less enhanced.

The decrease in N_2O along the vortex edge by 1 October is attributable to continuing descent in this region [e.g., *Manney et al.*, 1994]. Even though temperatures have risen above PSC thresholds, HNO_3 remains depleted (and does not recover substantially as long as the lower stratospheric vortex stays intact), implying the occurrence of denitrification. No such signature of widespread dehydration is seen at this level. Similar differences in the springtime distributions of HNO_3 and H_2O have been observed previously [e.g., *Manney et al.*, 1999]. Moreover, measurements from POAM (Polar Ozone and Aerosol Measurement) III also indicate atypically high stratospheric H_2O during this winter [G. Nedoluha, personal communication, 2004]. Lastly, chlorine has been almost completely deactivated, with only a hint of enhanced ClO remaining, whereas HCl is high throughout the vortex.

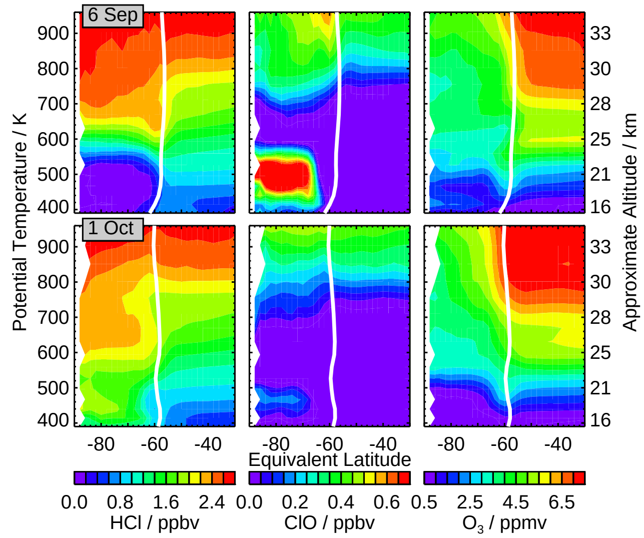

Figure 3. Equivalent latitude (EqL, the latitude enclosing the same area between it and the pole as a given PV contour)/potential temperature cross sections of MLS HCl, ClO, and O_3. Only ascending data are used for ClO. A contour of scaled PV [e.g., *Manney et al.*, 1994] outlines the vortex edge (white line).

The vertical extent of polar processing is shown in Figure 3. On 6 September, during the time of peak chlorine activation, almost all HCl has been removed inside the lower stratospheric vortex below $\sim$600 K. Very good correspondence is seen in the vertical extent of depleted HCl and enhanced ClO. Depletion in gas-phase HNO_3 (not shown), indicating PSC activity, also extends over a similar vertical range. That ClO enhancement more completely fills the vortex at lower altitudes is consistent with behavior observed in UARS MLS ClO data [*Santee et al.*, 2003]. The downward excursion of O_3 contours across the vortex edge in the lower stratosphere arises in part because in the southern hemisphere descent is strongest in this region [e.g., *Manney et al.*, 1994, 1999]. By 1 October HCl has recovered and nearly all ClO has disappeared above 500 K, although weak enhancement persists at lower altitudes. Comparing

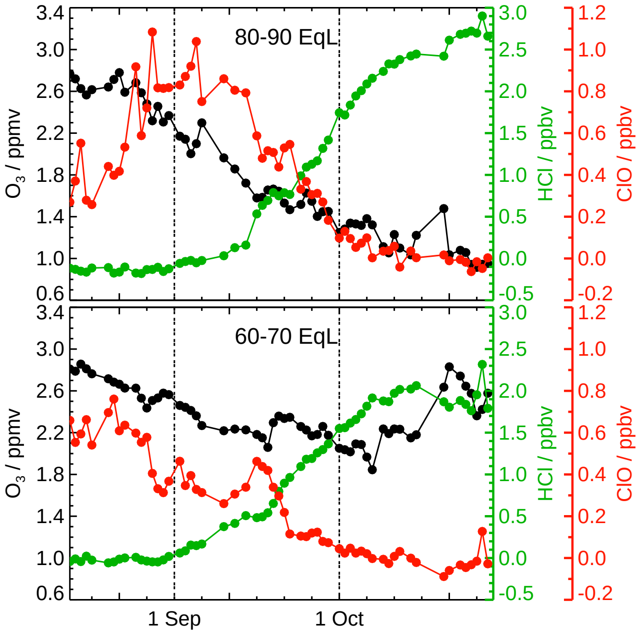

Figure 4. Time series of MLS HCl, ClO, and O_3 at 520 K. Daily means were calculated by binning the measurements into two 10°-wide EqL bands and averaging. Day-night differences are shown for ClO. Dots represent days for which retrievals are available; MLS made measurements on most days in this period, but not all data collected have been run through the data processing system.

the two O_3 panels illustrates the development of the lower stratospheric ozone hole over the month of September.

Figure 4 shows time series of 520 K MLS measurements binned into two equivalent latitude (EqL) bands representing the core and edge of the polar vortex. In the vortex core, ClO continues to increase until early September, reflecting the changing solar zenith angle conditions. ClO then declines rapidly and disappears by early October. HCl recovers very quickly in this region starting in mid-September. Rapid ozone loss begins in late August and levels off in early October. In contrast, near the vortex edge ClO reaches smaller maximum abundances and is relatively constant in mid-August, decreasing thereafter. HCl recovery starts earlier and is more gradual than at higher EqLs. The timing of the recovery, with almost all active chlorine converted back to HCl by mid-October, agrees well with that seen previously in ground-based infrared column measurements [*Liu et al.*, 1992; *Kreher et al.*, 1996]. Ozone loss, which most likely started in this region well before mid-August [e.g., *Lee et al.*, 2000], appears to be less severe than that in the vortex core, although it is also being compensated more by the stronger descent in this region [e.g., *Manney et al.*, 1994, 1995].

A broader view poleward of 30°S EqL is given in Fig-

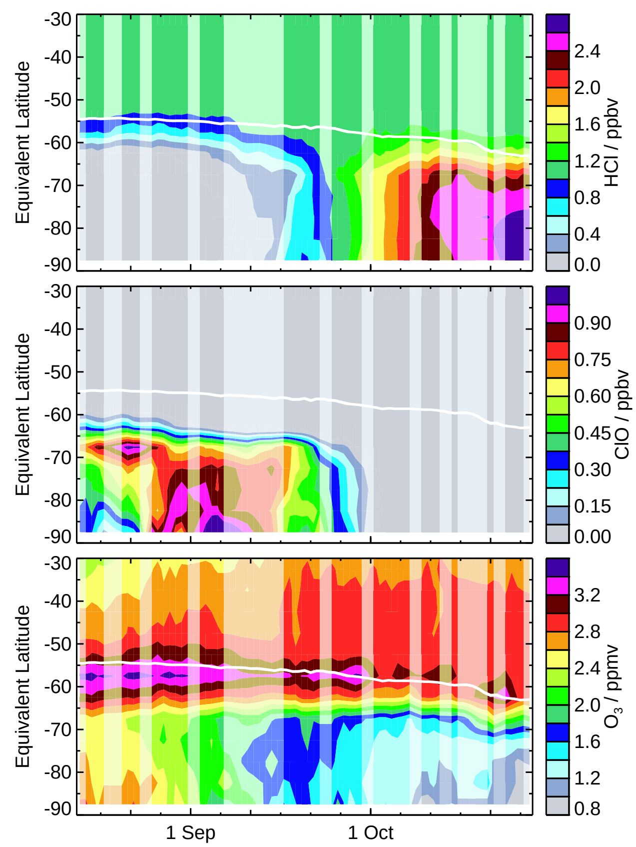

Figure 5. Time series of MLS HCl, ClO, and O_3 versus EqL at 520 K. Only ascending data are used for ClO. To fill in breaks arising from data gaps, Kalman smoothing has been applied to the daily values; paler colors denote regions where the estimated precision of the interpolated values is poor (see text). A PV contour (white line) demarks the vortex edge.

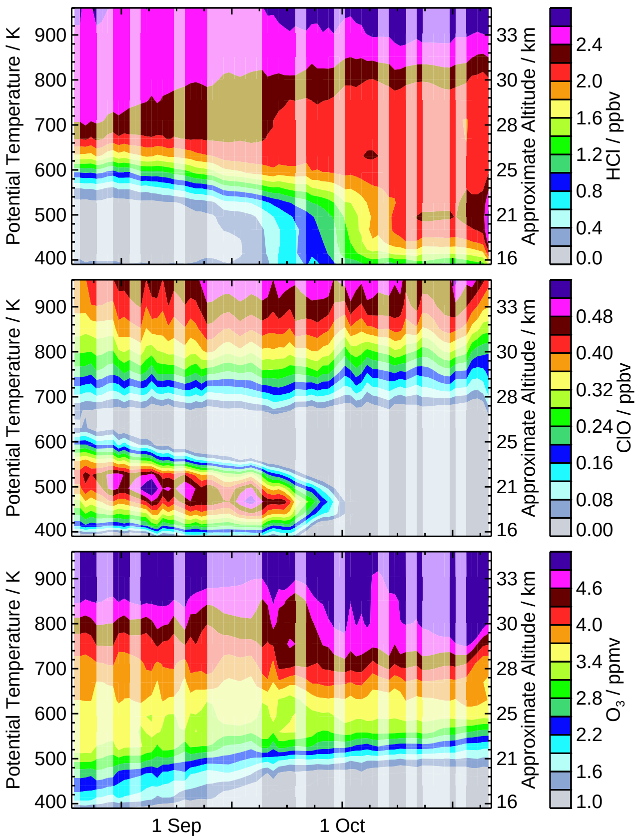

Figure 6. Time series of vortex-averaged MLS HCl, ClO, and O_3, calculated within the $1.4\times10^{-4}\,s^{-1}$ contour of scaled PV, as a function of potential temperature. Only ascending data are used for ClO.

ure 5. To enhance the clarity of this plot, short data gaps have been filled by running the daily averages through a Kalman smoother; paler colors denote regions where data are sparse or missing [see, e.g., *Santee et al.*, 2004]. The spatial and temporal extent of chlorine activation are consistent in the ClO and HCl fields. Inside the vortex, O_3 decreases steadily. In fact, O_3 continues to drop at the highest EqLs even after chlorine has been deactivated, which may indicate the onset of diabatic ascent in the vortex core [e.g., *Manney et al.*, 1994]. MLS H_2O and HNO_3 data (not shown) are also consistent with significant ascent in the vortex core by mid-October.

Vortex averages as a function of potential temperature and time (Figure 6) show that the vertical extent of ClO enhancement is consistent with that of HCl depletion, as is its decay over time. Figure 6 also shows the late-winter downward progression of the ClO profile peak, seen previously in UARS MLS [*Santee et al.*, 2003] and ground-based [*de Zafra et al.*, 1995; *Solomon et al.*, 2002] measurements. O_3 loss is clearly visible up to ~580 K but likely extends to higher altitudes; studies have indicated that chemical destruction takes place up to ~650 K but is at least partially compensated by the effects of downward transport above 520 K [e.g., *Manney et al.*, 1995].

New observations from MLS on Aura provide a much more complete picture of polar processing than was previously available. They appear to be consistent with current understanding of the dominant processes affecting stratospheric O_3 in the Antarctic late winter.

Acknowledgments. Y. Jiang and R. P. Thurstans are thanked for their help in producing the MLS animation, and S. A. Sena is thanked for making Figure 1. Work at the Jet Propulsion Laboratory, California Institute of Technology, was done under contract with the National Aeronautics and Space Administration.

References

de Zafra, R. L., J. M. Reeves, and D. T. Shindell, Chlorine monoxide in the Antarctic spring vortex, 1. Evolution of midday vertical profiles over McMurdo Station, 1993, *J. Geophys. Res.*, *100*, 13,999–14,007, 1995.

Douglass, A. R., et al., Interhemispheric differences in springtime production of HCl and $ClONO_2$ in the polar vortices, *J. Geophys. Res.*, *100*, 13,967–13,978, 1995.

Kreher, K., et al., Ground-based measurements of OClO and HCl in austral spring 1993 at Arrival Heights, Antarctica, *Geophys. Res. Lett.*, *23*, 1545–1548, 1996.

Lee, A. M., H. K. Roscoe, and S. Oltmans, Model and measurements show Antarctic ozone loss follows edge of polar night, *Geophys. Res. Lett.*, *27*, 3845–3848, 2000.

Liu, X., , et al., Measurements and model calculations of HCl column amounts and related parameters over McMurdo during the austral spring in 1989, *J. Geophys. Res.*, *97*, 20,795–20,804, 1992.

Manney, G. L., et al., On the motion of air through the stratospheric polar vortex, *J. Atmos. Sci.*, *51*, 2973–2994, 1994.

Manney, G. L., et al., Lagrangian transport calculations using UARS data. Part II: Ozone, *J. Atmos. Sci.*, *52*, 3069–3081, 1995.

Manney, G. L., et al., Polar vortex dynamics during spring and fall diagnosed using trace gas observations from the Atmospheric Trace Molecule Spectroscopy instrument, *J. Geophys. Res.*, *104*, 18,841–18,866, 1999.

Santee, M. L., et al., Chlorine deactivation in the lower stratospheric polar regions during late winter: Results from UARS, *J. Geophys. Res.*, *101*, 18,835–18,859, 1996.

Santee, M. L., et al., Variations and climatology of ClO in the polar lower stratosphere from UARS Microwave Limb Sounder measurements, *J. Geophys. Res.*, *108*, 4454, doi:10.1029/2002JD003335, 2003.

Santee, M. L., et al., Three-dimensional structure and evolution of stratospheric HNO_3 based on UARS Microwave Limb Sounder measurements, *J. Geophys. Res.*, *109*, D15306, doi:10.1029/2004JD004578, 2004.

Schoeberl, M. R., et al., Earth Observing System missions benefit atmospheric research, *EOS Trans. AGU*, *85*, 177, 181, 2004.

Solomon, P., et al., Measurements of stratospheric ClO over Antarctica in 1996–2000 and implications for ClO dimer chemistry, *Geophys. Res. Lett.*, *29*, 10.1029/2002GL015232, 2002.

Waters, J. W., et al., The UARS and EOS Microwave Limb Sounder (MLS) experiments, *J. Atmos. Sci.*, *56*, 194–218, 1999.

M. L. Santee (corresponding author), L. Froidevaux, N. J. Livesey, W. G. Read, M. J. Schwartz, and J. W. Waters, Jet Propulsion Laboratory, Mail Stop 183–701, 4800 Oak Grove Drive, Pasadena, CA 91109. (e-mail: mls@mls.jpl.nasa.gov)

G. L. Manney, Department of Natural Sciences, New Mexico Highlands University, Las Vegas, NM 87701.

H. C. Pumphrey, School of GeoSciences, The University of Edinburgh, Edinburgh EH9 3JZ, UK.

This preprint was prepared with AGU's LaTeX macros v4, with the extension package 'AGU^{++}' by P. W. Daly, version 1.5g from 1998/09/14.